Host–Guest Interaction Mediated Polymeric Assemblies: Multifunctional Nanoparticles for Drug and Gene Delivery

Jianxiang Zhang,[†] Hongli Sun,[†] and Peter X. Ma[†,‡,§,*]

[†]Department of Biologic and Materials Sciences, [‡]Macromolecular Science and Engineering Center, and [§]Department of Biomedical Engineering, University of Michigan, Ann Arbor, Michigan 48109

ABSTRACT Novel core–shell structured nanoassemblies are assembled by a β-cyclodextrin containing a positively charged host polymer and a hydrophobic guest polymer. The hydrophobic core of these types of assemblies serves as a nanocontainer to load and release the hydrophobic drugs, while the positively charged hydrophilic shell is able to condense the plasmid DNA and achieve its transfection/expression in osteoblast cells. These assemblies may be used as a new generation of multifunctional nanocarriers for simultaneous drug delivery and gene therapy.

KEYWORDS: host–guest interactions · polymer assemblies · multifunctional nanoparticles · drug delivery · gene delivery

Multifunctionalized nanocarriers are attractive in pharmaceutics, medical imaging, biomedical engineering, and gene therapy.[1] For instance, drug delivery, cell targeting, and/or multimodal imaging can be simultaneously achieved by multifunctional inorganic nanoparticles or nanocrystals, inorganic–organic hybrid nanoparticles, and polymeric assemblies.[2–9] Studies based on these versatile pharmaceutical nanocarriers have provided profound insights on the intracellular or *in vivo* distribution and valuable information on the spatial and temporal interactions of delivery carriers with cells and tissues as well as their intracellular interactions. In addition, multifunctional nanoparticles have also been employed to implement simultaneous gene delivery, drug delivery, and imaging.[6,10–14] Using cyanine dye (Cy5.5)-labeled magnetic nanoparticles conjugated to a synthetic small interfering RNA (siRNA) duplex, Moore and co-workers were able to achieve the *in vivo* transfer of siRNA and the simultaneous imaging of its accumulation in tumors by high-resolution magnetic resonance imaging and near-infrared *in vivo* optical imaging.[15] Proton-sponge-coated quantum dots were employed by Nie and Gao *et al.* for siRNA delivery and intracellular imaging.[16]

While these nanocarriers allow the real-time tracking and ultrastructural localization of the siRNA delivery system, combining drug delivery and gene therapy in one particle has the potential to enhance the transfection efficiency or to achieve a synergistic/combined effect of drug and gene therapies.[17–20] By co-delivering inflammatory suppressors and plasmid DNA (pDNA) through liposomes, Huang and co-workers developed a non-immunostimulatory gene vector (safeplex), which can inhibit the inflammatory toxicity induced by cationic lipids and CpG motif of pDNA.[21] Using cationic core–shell nanoparticles self-assembled from an amphiphilic copolymer, co-delivery of paclitaxel and pDNA/siRNA was achieved by Yang *et al.*[22] Both *in vitro* and *in vivo* studies demonstrated that these nanoparticles could suppress cancer growth more efficiently compared with a delivery system containing either drug or therapeutic gene alone. Recently, polymeric micelles based on polyethyleneimine-grafted poly(ε-caprolactone) have also been employed as the dual carriers of an anticancer drug and gene to achieve the synergistic effects.[23] Although only a few studies regarding multifunctional pharmaceutical nanocarriers based on polymers have been reported this far, such delivery systems already showed great potential for functioning as highly efficient and specialized carriers for drugs, genes, and diagnostic agents.

On the other hand, due to its excellent biocompatibility, β-cyclodextrin (β-CD) has been widely used as a host unit to construct

*Address correspondence to mapx@umich.edu.

Received for review September 11, 2009 and accepted January 22, 2010.

Published online January 29, 2010.
10.1021/nn901213a

delivery carriers.[24] Camptothecin-conjugated β-cyclodextrin-based polymers have been synthesized to assemble into nanoparticles for tumor therapy by Davis's group.[25,26] In addition, β-CD containing polycations were developed for siRNA delivery.[27,28] Most importantly, both delivery systems have been successfully developed to clinical trials. The aim of this contribution is to develop novel multifunctional polymeric nanoassemblies for simultaneous drug and gene delivery. The core−shell structured nanocarriers developed herein are assembled through a host−guest interaction by a β-cyclodextrin containing cationic polymer and a hydrophobic polymer. The hydrophobic core serves as a nanocontainer for lipophilic drugs, while the cationic shell can condense pDNA. Functioning as multifunctional nanovehicles, these polymeric assemblies can simultaneously deliver both hydrophobic drugs and genes.

RESULTS AND DISCUSSION

As a proof of concept, we selected a branched polyethyleneimine (PEI) as a scaffold polymer, onto which β-CDs were conjugated as the host units that can complex with a guest hydrophobic polymer to mediate the

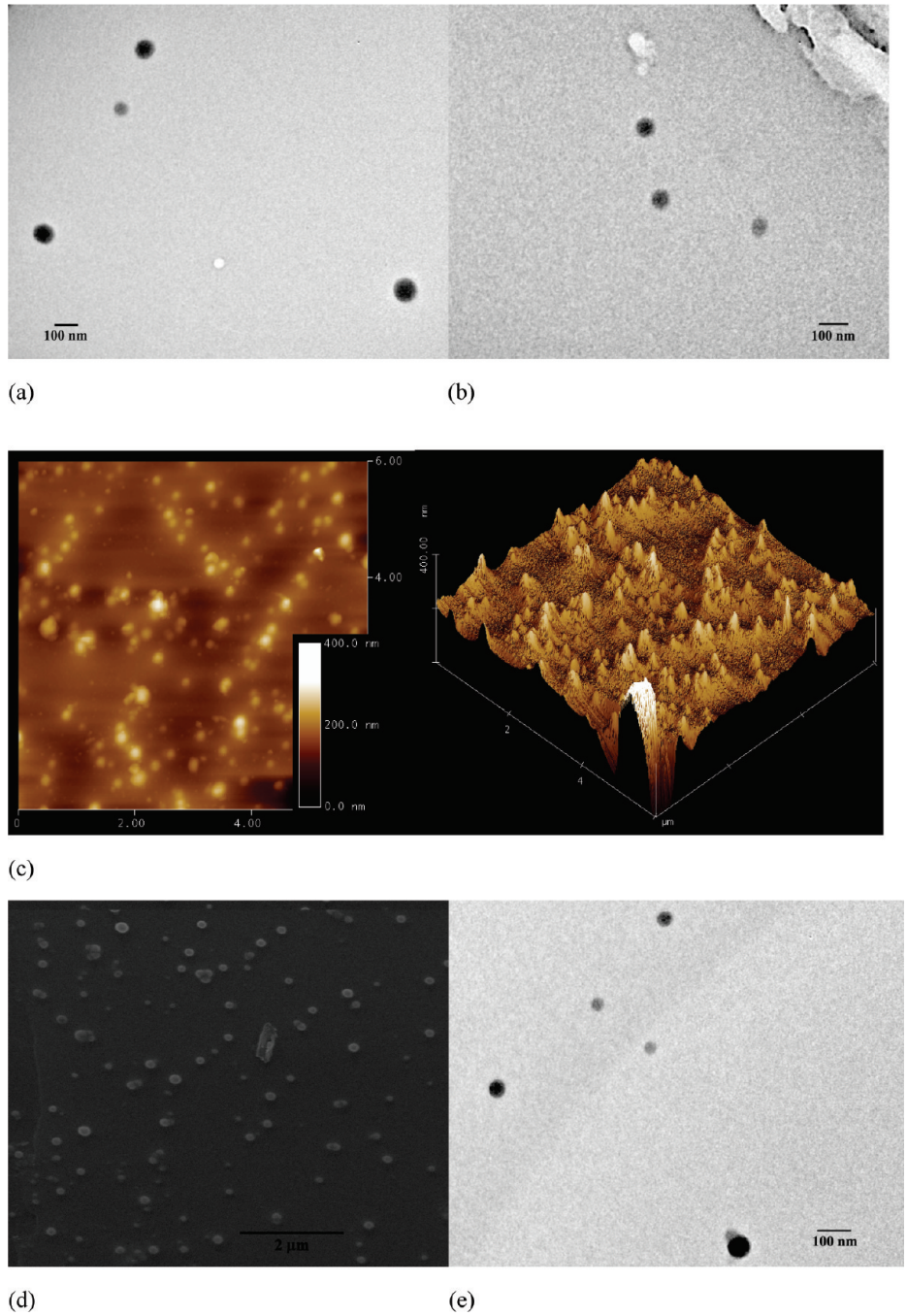

Figure 1. TEM images of assemblies based on PEI-CD/PBLA before (a) and after freeze-drying reconstitution (b); (c) AFM images of assemblies; (d) SEM image; and (e) TEM image of assemblies containing dexamethasone (DMS).

assembly process. By a nucleophilic substitution reaction between 6-monotosyl β-CD and an amino group of PEI, β-CD-conjugated PEI (PEI-CD) was synthesized. Figure S1b (Supporting Information) shows the ^{1}H NMR spectrum of PEI-CD. In addition to the chemical shift at 2.5−3.0 ppm, the appearance of signals at 3.4−4.0 and 5.1 ppm, which are characteristic signals of protons from β-CD, suggested the successful conjugation of β-CD units. Moreover, as shown in Figure S2a,b, absorption at 1033 cm^{-1} due to −C−O− groups increased significantly compared with that of PEI, which also verified the introduction of β-CD units onto the PEI scaffold. Calculation based on the ^{1}H NMR spectrum indicated that about 13 β-CD groups were conjugated onto each PEI chain. On the other hand, poly(β-benzyl L-aspartate) (PBLA), a hydrophobic polymer with flanking benzyl groups, was selected as a model guest polymer. The molecular weight of PBLA synthesized by a ring-opening polymerization was about 2000 as determined by a matrix-assisted laser desorption/ionization time-of-flight (MALDI-TOF) mass spectrometer.

By a modified dialysis procedure, assemblies based on PEI-CD/PBLA were prepared. A preliminary FT-IR measurement was performed to confirm the incorporation of the PBLA component into the assemblies. As shown in Supporting Information Figure S2c, in addition to absorptions due to PEI-CD, new peaks corresponding to PBLA appeared, especially that at 1735 cm^{-1}, which is a characteristic stretching vibration of carbonyl in PBLA. Accordingly, this result indicated the presence of PBLA component in the obtained assemblies. Unless stated otherwise, all of the following studies were based on the assemblies prepared by the formulation with a weight ratio (PEI-CD to PBLA) of 10:3. The morphology of assemblies was characterized using transmission electron microscopy (TEM), atomic force microscopy (AFM), and scanning electron microscopy (SEM). As shown in Figure 1a, spherical assemblies can be observed. Statistical analysis based on TEM images suggested that the average size was 95 nm. The spherical morphology of assemblies was further demonstrated by AFM and SEM images, which are illustrated in Figure 1c,d. The number-averaged size determined by dynamic light scattering (DLS) was 90.6 nm (Figure 2), and this result was consistent with TEM and SEM observation. The combination of TEM, AFM, and SEM results pointed to the conclusion that spherical nanoparticles can be assembled by PEI-CD in the presence of PBLA. Thus obtained nanoassemblies were stable enough to be characterized by AFM and SEM. In addition, by staining with phosphotungstic acid (PTA), we were able to directly observe the core−shell structure of PEI-CD/PBLA assemblies. As shown in Figure 3, a dark shell can be clearly observed. Since PTA preferentially stains hydrophilic microdomains, this dark shell should correspond to hydrophilic segments of PEI chains.

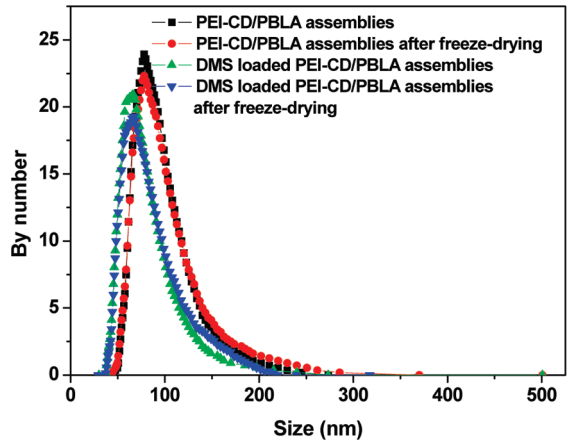

Figure 2. Size distribution of assemblies based on PEI-CD/PBLA with or without DMS.

Fluorescence measurement was then employed to provide information on the core of assemblies, and pyrene was used as a probe. Figure 4a shows the normalized emission spectra of pyrene in the presence of PEI-CD/PBLA-derived assemblies. The fluorescence band from 370 to 420 nm is the characteristic emission of excited pyrene monomer, while the broad band extending from 420 to 600 nm is ascribed to the pyrene excimer. With the increase in the assemblies' concentration, a significant enhancement in excimer intensity can be observed. Plots of concentration-dependent changes in intensity ratios of I_{338}/I_{333}, I_3/I_1, and I_E/I_M are shown in Figure 4b. Significant increase in the values of I_{338}/I_{333}, I_3/I_1, and I_E/I_M can be observed for pyrene as the concentration of PEI-CD/PBLA assemblies increased to a certain point. On the basis of I_3/I_1 data, a critical concentration of 0.04 mg/mL was obtained. No significant changes in I_E/I_M, however, were found in the case of β-CD (Supporting Information Figure S3). Furthermore, the values of I_3/I_1 for PEI-CD/PBLA assemblies are comparable with those of polymeric micelles based on polyethylene glycol-*block*-poly(β-benzyl L-aspartate) (PEG-*b*-PBLA), which were significantly larger than

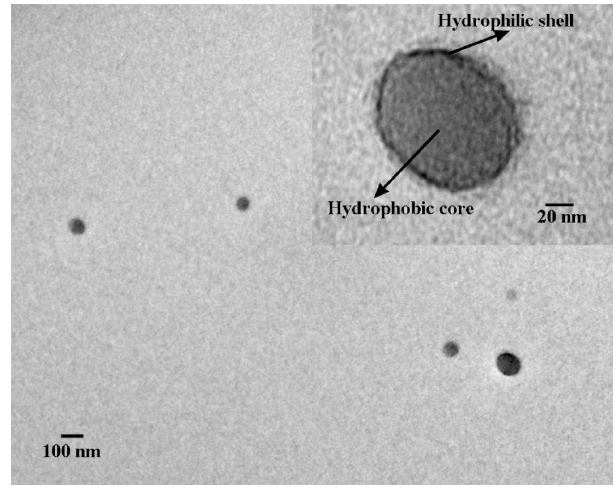

Figure 3. TEM image of PEI-CD/PBLA assemblies after staining with phosphotungstic acid.

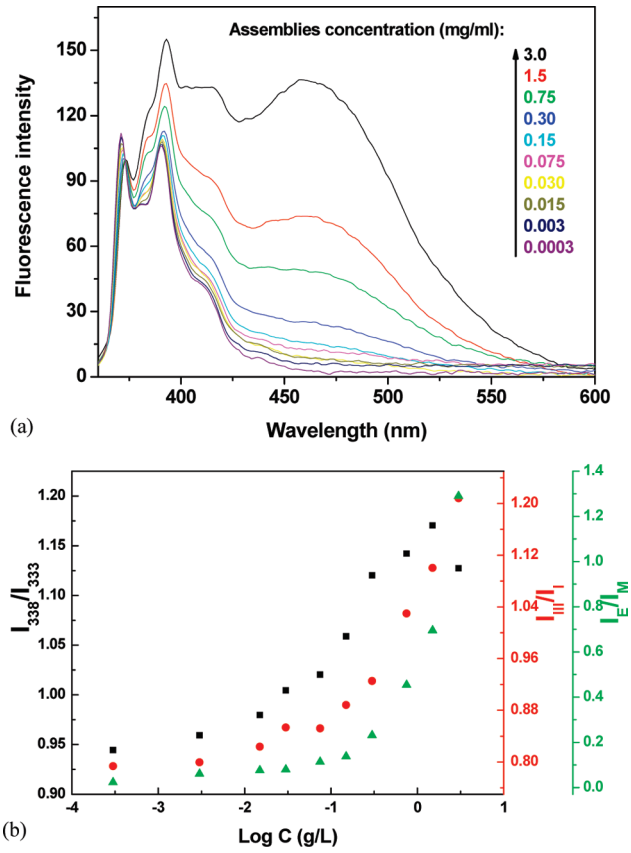

Figure 4. (a) Normalized emission spectra of pyrene in aqueous solutions containing various concentrations of PEI-CD/PBLA. (b) Plots of I_{338}/I_{333}, I_3/I_1, and I_E/I_M as a function of PEI-CD/PBLA concentration. I_{338}/I_{333} is the ratio of intensity at 338 nm to that at 333 nm in the (0,0) band of the pyrene excitation spectrum. I_3/I_1 is the intensity ratio between the third and first vibrational bands in the pyrene emission spectrum. I_E/I_M is the intensity ratio of the excimer (475 nm) to monomer (371 nm) in the emission spectrum; [pyrene] = 6.0×10^{-7} M.

those for β-CD. These observations indicated that assemblies based on PEI-CD/PBLA possessed a core similar to that of PEG-*b*-PBLA micelles. In other words, the core of PEI-CD/PBLA assemblies might be mainly composed of hydrophobic PBLA.

Further information on the microviscosity of the inner core of assemblies was provided by ^{1}H NMR and fluorescence anisotropy. As shown in Figure S1c (Supporting Information), no proton signals corresponding to PBLA can be observed for assemblies based on PEI-CD/PBLA in D_2O. However, signals at 7.3 and 5.0 ppm that are characteristic peaks of protons related to benzyl group are evident in DMSO-d_6. This indicates that the cores of these assemblies are mainly composed of PBLA chains with limited mobility, and therefore, these types of assemblies possess a rigid core. In the case of a fluorescence depolarization study, 1,6-diphenyl-1,3,5-hexatriene (DPH) was used as a fluorophore. The magnitude of *r* measured for DPH in an aqueous solution of PEI-CD/PBLA-based assemblies was about 0.26, which was even larger than that for PEG-*b*-PBLA-based micelles (r = 0.23 in this case). This result again suggested that the cores of assemblies based on PEI-CD/PBLA are essentially rigid.

As a summary, the above results suggested that core−shell structured nanoassemblies could be formed by PEI-CD in the presence of PBLA. A PBLA-rich microdomain formed the hydrophobic core, while positively charged PEI segments served as the hydrophilic shell. Since there is an inclusion interaction between the benzyl group and the CD unit, which has been well-documented,[29] this host−guest supramolecular interaction should contribute to the assembly of PEI-CD/PBLA. The assembly process is schematically illustrated in Scheme 1. With the introduction of PBLA into the aqueous solution of PEI-CD, the complexation interaction between the benzyl group and CD leads to the formation of pseudoamphiphilic polymers which are able to assemble into nanoparticles. Additional PBLA chains can also be incorporated considering the existence of hydrophobic interaction. In addition, as no peaks corresponding to PEI-CD chains can be observed from the DLS curve, almost all of the PEI-CD macromolecules might participate in the assembly process.

For assemblies to be used as drug/gene delivery carriers, the stability and dispersion behavior after the reconstitution from a freeze-dried formulation are important issues.[30] Frequently, the freeze-drying process may result in the formation of large aggregates, which in turn influences the therapeutic efficacy. As preliminary stability studies, the effect of freeze-drying/reconstitution on the size and morphology of assemblies was evaluated. Figure 1b shows the TEM image of PEI-CD/PBLA-based assemblies after freeze-drying and reconstitution. Spherical assemblies still can be observed when the freeze-dried samples were reconstituted in an aqueous medium. In addition, size distribution of assemblies shown in Figure 2 revealed that the freeze-drying and subsequent reconstitution had no significant effect on the particle size. The mean size of

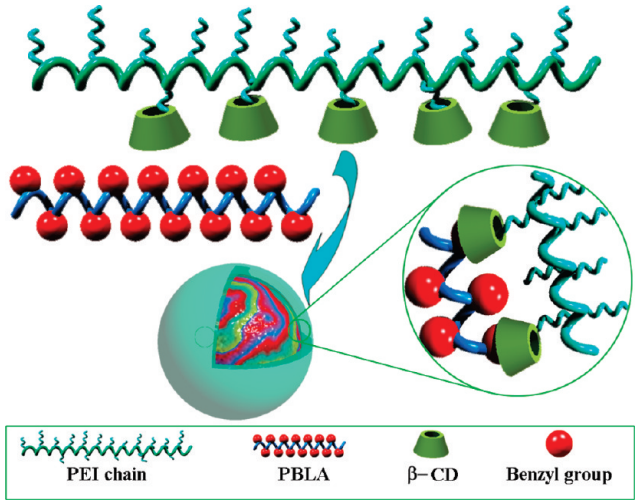

Scheme 1. Illustration of the core−shell nanoassemblies based on PEI-CD/PBLA by a host−guest interaction.

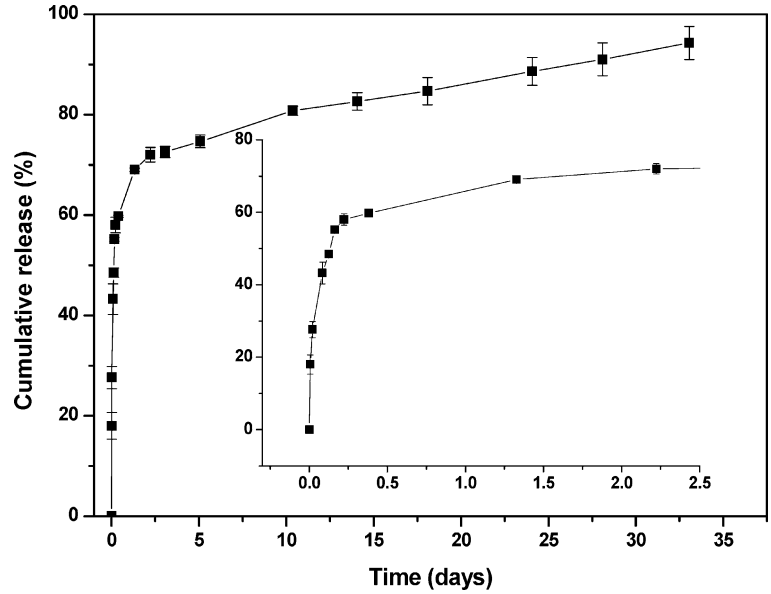

Figure 5. ***In vitro*** **DMS release profile from DMS containing PEI-CD/PBLA assemblies.**

assemblies after freeze-drying/reconstitution was 92.3 nm, which was essentially identical to that before freeze-drying (90.6 nm). This result indicates that these types of assemblies exhibit a good dispersion behavior after freeze-drying.

In order to address the capability of drug loading and release using PEI-CD/PBLA assemblies, dexamethasone (DMS), a highly hydrophobic steroidal anti-inflammatory drug, was selected. By a similar dialysis procedure, DMS containing assemblies were prepared. According to UV measurement, 5.8% DMS was loaded. The TEM image shown in Figure 1e suggested that the incorporation of DMS almost had no effect on the morphology of assemblies. Similar to the blank samples, a freeze-drying/reconstitution cycle had no significant impact on both particle size and size distribution of DMS containing assemblies (Figure 2). The number-average size before freeze-drying and after reconstitution was 74 and 78 nm, respectively. Figure 5 shows the cumulative release profile of DMS. A two-stage release behavior was observed: a rapid release within the first 2 days followed by a sustained release phase. It was also found that the release of DMS from PEI-CD/PBLA assemblies can be sustained for about 1 month. This result suggests that the core of PEI-CD/PBLA assemblies offers a nanocontainer to load and deliver a hydrophobic drug.

A titration experiment was performed to determine the pK_a values of both PEI-CD and PEI-CD/PBLA based on pH-dependent protonation curves. As shown in Figure S4 (Supporting Information), a similar two-stage protonation curve was observed for both PEI-CD and PEI-CD/PBLA, from which the pK_a values of the primary and secondary amino groups were determined to be 10.5 and 6.5, respectively. This result suggests that the presence of PBLA did not significantly affect the protonation behavior of PEI-CD. In addition, zeta-potential measurement revealed that the ζ-potential was 38.3 mV for PEI-CD/PBLA assemblies, indicating the positively charged surface of these nanoparticles. These results also support the core−shell structure of PEI-CD/PBLA assemblies as mentioned above.

As well-known, polyplexes (*i.e.*, the nanoparticles formed by electrostatic complexation of cationic polymers and DNA) have been widely employed as nonviral transfection vectors. Herein, polyplex-like nanovehicles were prepared by directly mixing pDNA with PEI-CD/PBLA assemblies at various weight ratios. Polyplex solutions thus obtained remained stable over a long-time storage, and no precipitate was observed over the entire range of weight ratios examined. To demonstrate the condensation capability of PEI-CD/PBLA nanoassemblies to pDNA, a gel retardation assay was performed. As shown in Figure 6a, the amount of migrating free pDNA gradually decreased with an increase in the weight ratio, indicating the complex formation between pDNA and PEI-CD/PBLA assemblies. Complete retardation of pDNA was achieved when the weight ratio increased to above 0.6. This was further confirmed by ethidium bromide (EtBr) exclusion assay. Whereas EtBr fluorescence intensity would be greatly enhanced by forming an intercalating complex with double-helical polynucleotides,[31] the complexation between DNA and a cationic polymer would result in a quenching of EtBr fluorescence. This characteristic of EtBr is frequently utilized to estimate the degree of pDNA condensation through complexation with a cationic polymer or positively charged nanoparticles.[32] As shown in Figure 6b, the fluorescence intensity of EtBr decreased with an increase in the weight ratio, which leveled off when the weight ratio was above 0.7. This decreased fluorescence is consistent with the gradual complexation of PEI-CD/PBLA assemblies with pDNA,

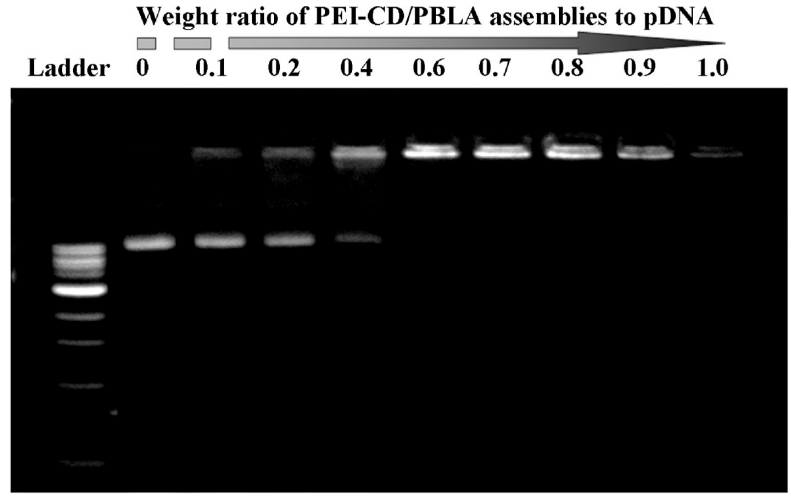

(a)

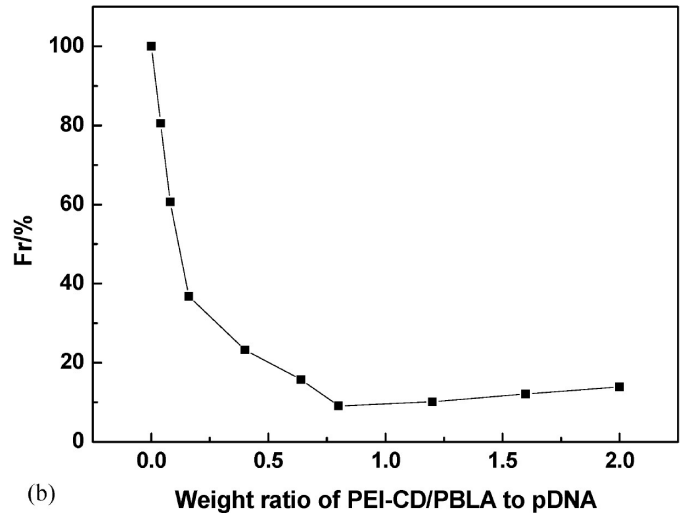

(b)

Figure 6. (a) Gel retardation assay of PEI-CD/PBLA assemblies and pDNA. (b) Relative fluorescence intensity (Fr) of EtBr in solution with pDNA and PEI-CD/PBLA assemblies at various weight ratios.

inhibiting the intercalation of EtBr into pDNA as a result of coil-to-globule transition of pDNA.[33] Note that the apparent end point of the coil-to-globule transition, evaluated based on EtBr exclusion, was consistent with the result of the gel retardation assay shown in Figure 6a.

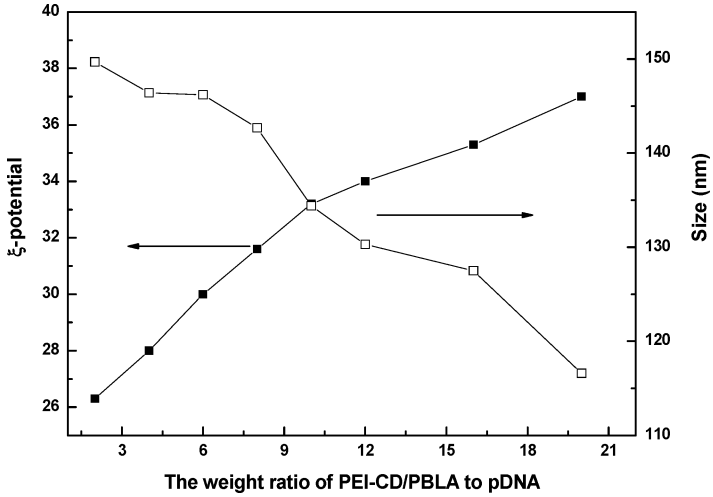

Figure 7. Zeta-potential and particle size of polyplexes based on PEI-CD/PBLA assemblies and pDNA with various weight ratios.

According to the above results of gel retardation as well as EtBr exclusion assays, pDNA could be essentially complexed with PEI-CD/PBLA assemblies to form a condensed structure when the weight ratio was higher than 0.6. To gain insight into the physicochemical properties of these complexes, DLS and ζ-potential measurements were then performed. As can be seen from Figure 7, the introduction of pDNA resulted in an increase in particle size (compare with Figure 2). However, increase in the weight ratio of PEI-CD/PBLA to pDNA led to a decrease in particle size. When the weight ratio increased from 2 to 20, the mean size decreased from 150 to 116 nm. As suggested by previous studies, this phenomenon was attributed to the formation of nonstoichiometric complexes.[33,34] Zeta-potential was significantly increased with the increase in the weight ratio of PEI-CD/PBLA to pDNA. For formulation

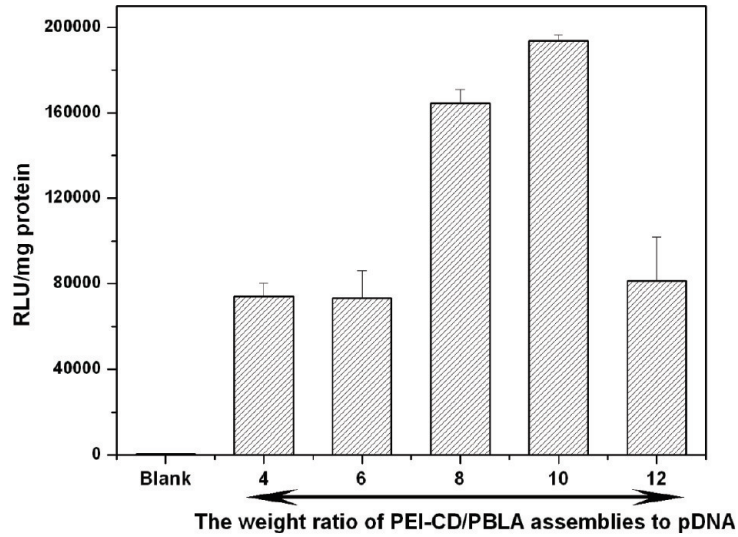

(a)

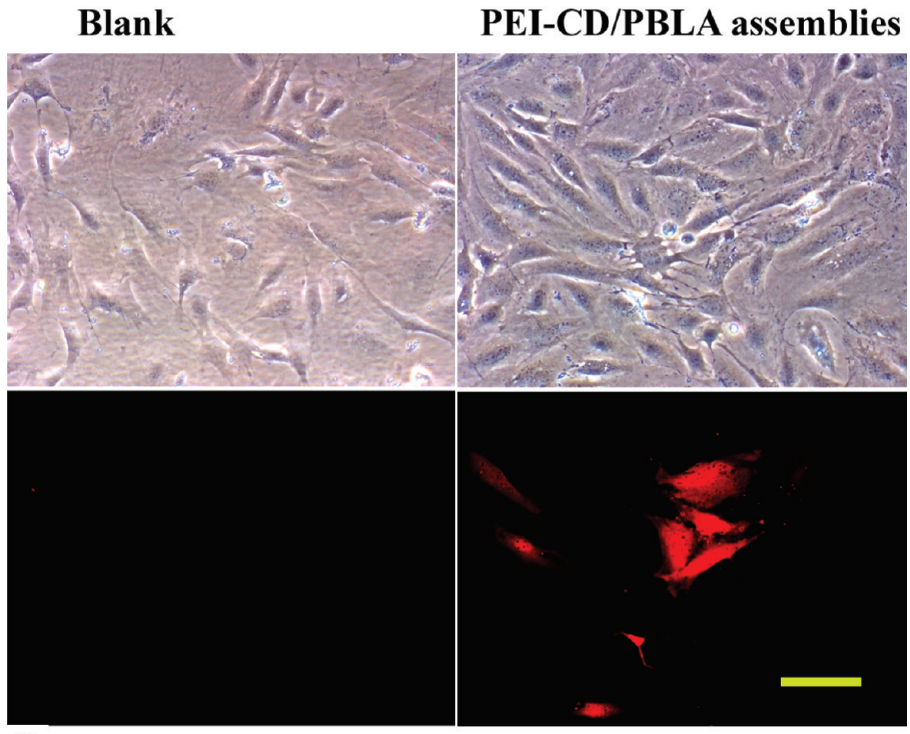

(b)

Figure 8. (a) *In vitro* transfection of the luciferase gene into osteoblast cells by PEI-CD/PBLA nanoassemblies. Luciferase activity (RLU) was quantified using a luminometer 48 h after cells were transfected. Results were normalized to total cell protein. All samples were run in triplicate and on three or more separate occasions. (b) Transfected cells were viewed by a fluorescence microscope (Nikon Eclipse 50i microscope) 48 h after transfection. Excitation was performed with green light. Polyplexes with the weight ratio of PEI-CD/PBLA to pDNA of 8 were employed. The scale bar represents 100 μm.

with a weight ratio of 20:1, ζ-potential was about 37, which was close to that of blank PEI-CD/PBLA assemblies. A similar phenomenon was observed previously for polyion complex (PIC) micelles based on oppositely charged polyelectrolytes.[33,35]

In vitro transfection experiment was performed with MC3T3-E1 osteoblast cells using the polyplexes prepared at various weight ratios. Although both the retardation and EtBr exclusion assay suggested that a complete condensation of pDNA was achieved when the weight ratio was above 0.6, effective transfection was not observed for formulations with a weight ratio slightly higher than 0.6. An appreciable increase in the transfection efficiency in the region of weight ratio ≥4 was observed, as shown in Figure 8a. This trend of increased gene transfection with the weight ratio was correlated with the increase in ζ-potential of polyplexes, as shown in Figure 7. Nevertheless, further increase in weight ratio may lead to a decrease in transfection. Luciferase activity reached a maximum at a weight ratio of

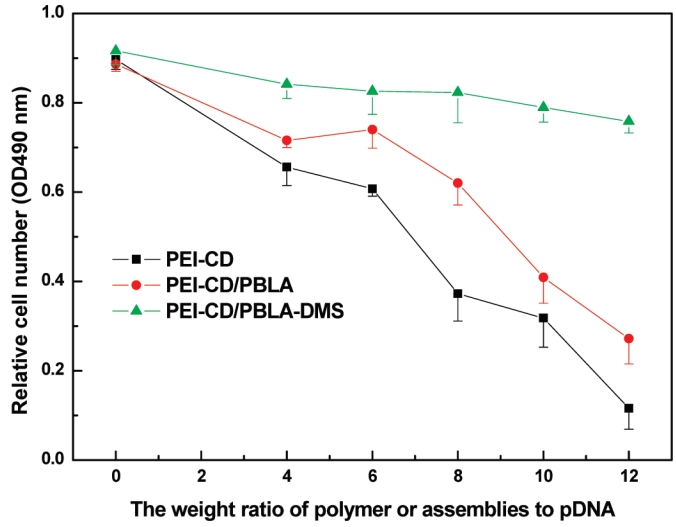

Figure 9. Cytotoxicity of PEI-CD/PBLA assemblies and DMS containing assemblies against osteoblast cells. After incubation for 24 h with the solutions of different polyplexes, the cell viability was detected using a Promega CellTiter 96 Aqueous one solution cell proliferation assay. The experiment was performed in triplicate.

10. In this case, intense red fluorescence can be observed for the cultured cells transfected with polyplexes based on PEI-CD/PBLA assemblies, while almost no transfected cells were found for the control group (Figure 8b), indicating the former to have transfected a significant number of cells and resulted subsequent gene expression. However, it should be noted that the transfection efficiency of our polyplexes was lower than that based on PEI alone at this moment. Further optimizing the delivery system by tailoring PEI-CD structure as well as modulating the assemblies' composition is necessary to increase the transfection activity while keeping lower cytotoxicity at the same time. Polyplexes based on DMS containing assemblies (the weight ratio of assemblies to pDNA was 10:10) were also prepared for transfection. Physicochemical characterization indicated that the loading of DMS had no influence on the resultant polyplexes compared with those based on the blank assemblies of the same formulation. A slight increase in transfection efficiency was observed for DMS containing polyplexes compared to the counterpart without DMS. This enhancement should be related to the DMS-induced dilation of nuclear pore complexes.[36] The increased nuclear translocation of macromolecules and nanoparticles by DMS has also been confirmed by other researchers.[37,38]

The low cytotoxicity of vectors is a crucial aspect for successful nonviral gene delivery. In this study, the cytotoxicity of polyplexes was evaluated by cell proliferation assay under the same conditions used for gene transfection. As shown in Figure 9, in comparison with PEI-CD, PEI-CD/PBLA assemblies showed low cytotoxicity. Interestingly, the cytotoxicity was drastically lowered for assemblies loaded with DMS. As an anti-inflammatory and immunosuppressive drug, DMS can inhibit proinflammatory cytokines such as tumor necrosis factor α (TNF-α) and antagonize the activation of the NF-κB pathway by direct and indirect mechanisms.[39] Through this way, DMS has been reported to efficiently decrease the inflammatory toxicity of lipoplexes.[21] For the first time, our study demonstrated that DMS can also decrease the cytotoxicity of nanocarriers based on PEI derivatives.

CONCLUSIONS

In summary, this study demonstrated the possibility of assembling nanocarriers based on a β-CD containing polyelectrolyte and a hydrophobic polymer, a process mediated by host−guest interaction between β-CD and the hydrophobic group. Assemblies formed through this protocol exhibited a core−shell architecture. The hydrophobic core mainly composed of the hydrophobic polymer can serve as a nanocontainer to accommodate and sustain the release of hydrophobic drugs. The hydrophilic shell of the positive segment can condense pDNA. Polyplexes thus constructed can achieve the transfection and gene expression of a plasmid DNA. These types of assemblies can simultaneously deliver both small molecular drugs and therapeutic macromolecules including proteins, DNA, and siRNA. Furthermore, due to the presence of functionally active amine groups at the periphery, additional functionalities such as stealthy and targeting capability can be conferred to these assemblies by further chemical decoration.

EXPERIMENTAL SECTION

Materials. L-Aspartic acid β-benzyl ester was purchased from Sigma (St. Louis, MO). Triphosgene was obtained from Fisher (USA). β-Benzyl-L-aspartate *N*-carboxyanhydride (BLA-NCA) was synthesized according to literature.[40] Pyrene (≥99%) and β-cyclodextrin (β-CD, ≥98%) were purchased from Sigma-Aldrich Co. (USA) and used as received. The method established by Baussanne *et al.* was employed to synthesize mono-6-(*p*-tosyl)-β-CD.[41] Dexamethasone (DMS), 1,6-diphenyl-1,3,5-hexatriene (DPH), and branched polyethyleneimine (PEI) with M_w of 25 000 were purchased from Sigma (St. Louis, MO).

Synthesis of β-Cyclodextrin-Conjugated Polyethyleneimine (PEI-CD). Branched PEI (1.5 g) was dissolved in 15 mL of DMSO, into which 10 mL of DMSO containing 1.5 g of mono-6-(*p*-tosyl)-β-CD was added. The reaction was performed at 75 °C for 5 days, and then the polymer was purified by dialysis.

Synthesis of Poly(β-benzyl L-aspartate) (PBLA). PBLA was synthesized according to ref 42. Briefly, 1.5 g of BLA-NCA was dissolved in 30 mL of anhydrous dioxane at −30 °C, into which an appropriate amount of *n*-hexylamine was added to achieve a molar ratio of monomer to initiator of 20:1. Polymerization was performed at room temperature (22 °C) for 5 days. After being precipitated from diethyl ether, the polymer was dissolved in dichloromethane and precipitated from diethyl ether again. The resultant powder was dried under vacuum. The number-average molecular weight determined by matrix-assisted laser desorption/ionization time-of-flight (MALDI-TOF) mass spectrometer is about 2000.

Polymer Characterization. ^{1}H NMR spectra were recorded on a Varian INOVA-400 spectrometer operating at 400 MHz. The MALDI-TOF mass spectrum of PBLA was acquired with a Waters Micromass TofSpec-2E run in a linear mode. Dithranol (purchased from Aldrich Chemical) was used as a matrix and tetrahydrofuran as a solvent for both matrix and polymer. The dried-droplet method was employed in sample preparation.[43] FT-IR spectra were recorded on a Perkin-Elmer FT-IR spectrometer (Spectrum GX).

Preparation of Assemblies Based on PEI-CD/PBLA. A modified dialysis procedure was used to prepare assemblies or DMS containing assemblies based on PEI-CD and PBLA. In brief, 3.0 mg of PBLA dissolved in 1.0 mL of DMSO was gradually added into 2.0 mL of aqueous solution of PEI-CD (10.0 mg/mL) under sonication. The mixture solution thus obtained was dialyzed against deionized water for 24 h at room temperature. The outer aqueous solution was renewed every 2 h. For the preparation of DMS containing assemblies, 3.0 mg of PBLA and 3.0 mg of DMS were dissolved in 1.0 mL of DMSO, which was added dropwise into 2.0 mL of deionized water containing 20 mg of PEI-CD under bath sonication, and then dialysis was performed. For all of the assemblies, characterization was performed after the aqueous solution was filtered through a 0.45 μm syringe filter.

Fluorescence Measurements. Using pyrene as a fluorophore, steady-state fluorescence spectra were measured on JASCO FP-6200 fluorescence spectrophotometer with a slit width of 5 nm for both excitation and emission. All spectra were run on air-equilibrated solutions. For fluorescence emission spectra, excitation wavelength was set at 339 nm, and for excitation spectra, the emission wavelength was 390 nm. The scanning rate was set at 125 nm/min. All tests were carried out at 25 °C. Sample solutions were prepared as described previously.[44] In brief, aqueous copolymer solutions containing pyrene (6.0×10^{-7} M) were incubated at 50 °C for 12 h and subsequently allowed to cool overnight to room temperature.

Fluorescence anisotropy (r) was determined with a Fluoromax-2 fluorimeter equipped with an autopolarizer accessory. The monochromator slits were set at 5.0 nm. 1,6-Diphenyl-1,3,5-hexatriene (DPH) was used as a fluorescence probe. The excitation wavelength was 360 nm, while the emission wavelength was 430 nm. The fluorescence anisotropy was calculated according to the relationship $r = (I_{VV} - GI_{VH})/(I_{VV} + 2GI_{VH})$, where $G = I_{VH}/I_{HH}$ is an instrumental correction factor and I_{VV}, I_{VH}, I_{HV}, and I_{HH} refer to the emission intensities polarized in the vertical or horizontal detection planes (second subindex) upon excitation with either vertically or horizontally polarized light (first subindex).[45] To prepare sample solutions, a known amount of DPH in methanol was added to 10.0 mL volumetric flasks and the methanol was evaporated. To each flask was then added a stock sample solution, which was heated at 50 °C for 12 h and cooled overnight to room temperature. The DPH concentration was kept at 1.0×10^{-6} M. The assemblies' concentration was 5 mg/mL.

Morphology Study. Transmission electron microscopy (TEM) observation was carried out on a JEOL-3011 high-resolution electron microscope operating at an acceleration voltage of 300 kV. Samples were prepared at 25 °C by dipping the grid into the aqueous solution of assemblies, and extra solution was blotted with filter paper. After the water was evaporated at room temperature for several days, samples were observed directly without any staining. Formvar-coated copper grids, stabilized with evaporated carbon film, were used. Atomic force microscopy (AFM) observation was carried out on a NanoScope IIIa-Phase atomic force microscope connected to a NanoScope IIIa controller using an EV scanner. Samples were prepared by drop-casting the dilute solution onto freshly cleaved mica. All of the images were acquired under a tapping mode. Scanning electron microscopy (SEM) images were taken on a field emission scanning electron microscope (XL30 FEG, Phillips) after a gold layer was coated using a sputter coater (Desk-II, Denton vacuum Inc., Moorstown, NJ) for 100 s. Samples were prepared by coating aqueous solution of assemblies onto freshly cleaved mica, and water was evaporated at room temperature under normal pressure.

Potentiometric Titration. PEI-CD or PEI-CD/PBLA assemblies were dissolved in 20 mL of 0.01 N HCl and titrated with 0.01 N NaOH. The pH values of the solution were determined by a pH meter (Orion 320, Thermo Electron Corporation).

***In Vitro* Release Study.** Five milligrams of lyophilized samples of assemblies containing DMS was dissolved into 0.5 mL of deionized water and placed into dialysis tubing, which was immerged into 30 mL of PBS (0.1 M, pH 7.4). At a predetermined time interval, 4.0 mL of release medium was withdrawn, and fresh PBS was added. DMS concentration in the release buffer was determined by UV at 265 nm.

Dynamic Light Scattering (DLS) and ζ-Potential Measurements. DLS and ζ-potential measurements for the assemblies and assemblies/pDNA-based polyplexes in aqueous solutions were performed with a Malvern Zetasizer Nano ZS instrument at 25 °C.

Cells and Plasmid DNA (pDNA). MC3T3-E1 (clone 26) cells were cultured in alpha minimum essential medium (α-MEM) supplemented with 10% bovine serum, 100 U/mL penicillin and 100 μg/mL streptomycin in a humidified incubator at 37 °C with 5% CO_2.[46] The pGL3-control vector (Promega, Madison, WI), containing the luciferase gene driven by the SV40 promoter and enhancer was grown in DH5 α *Escherichia coli* and purified using Qiagen Hispeed plasmid purification kit. The ratio of absorbance at 260 and 280 nm was 1.8 or greater.

Gel Retardation Analysis. PEI-CD or assembly sample was dissolved in 10 mM Tris-HCl (pH 7.4) buffer at 1.0 mg/mL, which was then mixed with pDNA in 10 mM Tris-HCl (pH 7.4) (1.0 mg/mL) at varying mass ratios. The mixed solution was diluted to 20 μg pDNA/mL by 10 mM Tris-HCl (pH 7.4), followed by an overnight incubation at room temperature. Ten microliters of each sample (200 ng pDNA) was electrophoresed at 100 V for 0.5 h on a 0.8% agarose gel in 20 mM Tris-acetic acid buffer containing 10 mM sodium acetic acid (pH 7.8); pDNA in the gel was visualized by EtBr (0.5 μg/mL) staining.

Dye Exclusion Assay. Dye exclusion experiment was performed according to literature.[32] Polyplex solutions prepared by mixing pDNA and PEI-CD/PBLA assemblies at different weight ratios were diluted to 10 μg/mL pDNA with ethidium bromide (EtBr, 4.0 μg/mL) in 10 mM Tris-HCl (pH 7.4) buffer. The sample solutions were incubated at room temperature overnight. The fluorescence intensity of the samples at 590 nm (excitation at 510 nm) was measured using a spectrofluorometer (Fluoromax-2 fluorimeter). The relative fluorescence intensity was calculated as $F_r = (F_s - F_0)/(F_f - F_0)$, in which F_s, F_f, and F_0 represent the fluorescence intensity of the samples, free pDNA, and background, respectively.

Polyplex Formation and Transfection. PEI-CD was dissolved in 20 mM HEPES with 150 mM NaCl (pH 7.3). Polyplexes were prepared by adding 50 μL of PEI-CD of varying concentrations to an equal volume of 1.0 μg of pDNA (in Tris-HCl buffer) to achieve the desired polymer/pDNA weight ratio. Polyplexes were then incubated at room temperature for 20 min. Cells were plated in 24-well plates at high density 24 h prior to transfection. Immediately before transfection, the growth medium was replaced with serum-free medium (500 μL/well), and 50 μL polyplex solution (1.0 μg plasmid/well) was added to each well. Transfection medium was replaced with fresh growth medium 5 h post-transfection. Luciferase expression was quantified 48 h later using a Promega luciferase assay system. Luciferase activity was measured in relative light units (RLU) using luminometer. Results were normalized to total cell protein as determined using a Pierce Micro BCA protein assay. All samples were run in triplicate and on three or more separate occasions. By the similar protocol, polyplexes based on PEI-CD/PBLA assemblies and DMS containing assemblies were evaluated.

Cytotoxicity Determination. The cytotoxicity of polyplexes was tested using a Promega CellTiter 96 AQueous One Solution cell proliferation assay. Briefly, cells were plated in 24-well plates at 1×10^5 cells/well and cultured for 24 h. Polyplexes were then added to each well. After 24 h of incubation, the medium was changed to fresh medium (400 μL/well) and 40 μL of MTS solution was added to each well. The plates were then incubated in a 5% CO_2 incubator at 37 °C for 1 h. The absorbance of the medium from each well was read at 490 nm with an ELISA plate reader. The experiment was performed in triplicate.

Acknowledgment. The authors would like to acknowledge the financial support from the NIH (NIDCR DE015384 and DE017689). The authors gratefully acknowledge Prof. K Kuroda for making the fluorescence spectrophotometer available, and Prof. N.A. Kotov for making DLS instrument available for this project.

Supporting Information Available: ^{1}H NMR, FT-IR, and fluorescence spectra and titration curves. This material is available free of charge via the Internet at http://pubs.acs.org.

REFERENCES AND NOTES

1. Torchilin, V. P. Multifunctional Nanocarriers. *Adv. Drug Delivery Rev.* **2006**, *58*, 1532–1555.
2. Kim, J.; Park, S.; Lee, J. E.; Jin, S. M.; Lee, J. H.; Lee, I. S.; Yang, I.; Kim, J. S.; Kim, S. K.; Cho, M. H.; Hyeon, T. Designed Fabrication of Multifunctional Magnetic Gold Nanoshells and Their Application to Magnetic Resonance Imaging and Photothermal Therapy. *Angew. Chem., Int. Ed.* **2006**, *45*, 7754–7758.
3. Kim, J. S.; Rieter, W. J.; Taylor, K. M. L.; An, H. Y.; Lin, W. L.; Lin, W. B. Self-Assembled Hybrid Nanoparticles for Cancer-Specific Multimodal Imaging. *J. Am. Chem. Soc.* **2007**, *129*, 8962–8963.
4. Huang, C. K.; Lo, C. L.; Chen, H. H.; Hsiue, G. H. Multifunctional Micelles for Cancer Cell Targeting, Distribution Imaging, and Anticancer Drug Delivery. *Adv. Funct. Mater.* **2007**, *17*, 2291–2297.
5. Li, Y. Y.; Cheng, H.; Zhang, Z. G.; Wang, C.; Zhu, J. L.; Liang, Y.; Zhang, K. L.; Cheng, S. X.; Zhang, X. Z.; Zhuo, R. X. Cellular Internalization and *In Vivo* Tracking of Thermosensitive Luminescent Micelles Based on Luminescent Lanthanide Chelate. *ACS Nano* **2008**, *2*, 125–133.
6. Liong, M.; Lu, J.; Kovochich, M.; Xia, T.; Ruehm, S. G.; Nel, A. E.; Tamanoi, F.; Zink, J. I. Multifunctional Inorganic Nanoparticles for Imaging, Targeting, and Drug Delivery. *ACS Nano* **2008**, *2*, 889–896.
7. Kim, J.; Lee, J. E.; Lee, S. H.; Yu, J. H.; Lee, J. H.; Park, T. G.; Hyeon, T. Designed Fabrication of a Multifunctional Polymer Nanomedical Platform for Simultaneous Cancer-Targeted Imaging and Magnetically Guided Drug Delivery. *Adv. Mater.* **2008**, *20*, 478–483.
8. Rieter, W. J.; Kim, J. S.; Taylor, K. M. L.; An, H. Y.; Lin, W. L.; Tarrant, T.; Lin, W. B. Hybrid Silica Nanoparticles for Multimodal Imaging. *Angew. Chem., Int. Ed.* **2007**, *46*, 3680–3682.
9. Kim, S.; Ohulchanskyy, T. Y.; Pudavar, H. E.; Pandey, R. K.; Prasad, P. N. Organically Modified Silica Nanoparticles Co-encapsulating Photosensitizing Drug and Aggregation-Enhanced Two-Photon Absorbing Fluorescent Dye Aggregates for Two-Photon Photodynamic Therapy. *J. Am. Chem. Soc.* **2007**, *129*, 2669–2675.
10. Qi, L. F.; Gao, X. H. Quantum Dot−Amphipol Nanocomplex for Intracellular Delivery and Real-Time Imaging of siRNA. *ACS Nano* **2008**, *2*, 1403–1410.
11. Nehilla, B. J.; Allen, P. G.; Desai, T. A. Surfactant-Free, Drug-Quantum-Dot Coloaded Poly(lactide-*co*-glycolide) Nanoparticles: Towards Multifunctional Nanoparticles. *ACS Nano* **2008**, *2*, 538–544.
12. Ghosh, P. S.; Kim, C. K.; Han, G.; Forbes, N. S.; Rotello, V. M. Efficient Gene Delivery Vectors by Tuning the Surface Charge Density of Amino Acid-Functionalized Gold Nanoparticles. *ACS Nano* **2008**, *1*, 2213–2218.
13. Al-Jamal, W. T.; Al-Jamal, K. T.; Tian, B.; Lacerda, L.; Bomans, P. H.; Frederik, P. M.; Kostarelos, K. Lipid-Quantum Dot Bilayer Vesicles Enhance Tumor Cell Uptake and Retention *In Vitro* and *In Vivo*. *ACS Nano* **2008**, *2*, 408–418.
14. Farokhzad, O. C.; Langer, R. Impact of Nanotechnology on Drug Delivery. *ACS Nano* **2009**, *3*, 16–20.
15. Medarova, Z.; Pham, W.; Farrar, C.; Petkova, V.; Moore, A. *In Vivo* Imaging of siRNA Delivery and Silencing in Tumors. *Nat. Med.* **2007**, *13*, 372–377.
16. Yezhelyev, M. V.; Qi, L. F.; O'Regan, R. M.; Nie, S. M.; Gao, X. H. Proton-Sponge Coated Quantum Dots for siRNA Delivery and Intracellular Imaging. *J. Am. Chem. Soc.* **2008**, *130*, 9006–9012.
17. Malone, R. W.; Hickman, M. A.; Lehmann-Bruinsma, K.; Sih, T. R.; Walzem, R.; Carlson, D. M.; Powell, J. S. Dexamethasone Enhancement of Gene Expression after Direct Hepatic DNA Injection. *J. Biol. Chem.* **1994**, *269*, 29903–29907.
18. Zhang, X. H.; Collins, L.; Sawyer, G. J.; Dong, X. B.; Qiu, Y.; Fabre, J. W. *In Vivo* Gene Delivery *via* Portal Vein and Bile Duct to Individual Lobes of the Rat Liver Using a Polylysine-Based Nonviral DNA Vector in Combination with Chloroquine. *Hum. Gene Ther.* **2001**, *12*, 2179–2190.
19. Kishida, T.; Asada, H.; Itokawa, Y.; Yasutomi, K.; Shin-Ya, M.; Gojo, S.; Cui, F. D.; Ueda, Y.; Yamagishi, H.; Imanishi, J.; Mazda, O. Electrochemo-Gene Therapy of Cancer: Intratumoral Delivery of Interleukin-12 Gene and Bleomycin Synergistically Induced Therapeutic Immunity and Suppressed Subcutaneous and Metastatic Melanomas in Mice. *Mol. Ther.* **2003**, *8*, 738–745.
20. Janat-Amsbury, M. M.; Yockman, J. W.; Lee, M.; Kern, S.; Furgeson, D. Y.; Bikram, M.; Kim, S. W. Combination of Local, Nonviral IL12 Gene Therapy and Systemic Paclitaxel Treatment in a Metastatic Breast Cancer Model. *Mol. Ther.* **2004**, *9*, 829–836.
21. Liu, F.; Shollenberger, L. M.; Huang, L. Non-immunostimulatory Nonviral Vectors. *FASEB J.* **2004**, *18*, 1779–1781.
22. Wang, Y.; Gao, S. J.; Ye, W. H.; Yoon, H. S.; Yang, Y. Y. Co-delivery of Drugs and DNA from Cationic Core−Shell Nanoparticles Self-Assembled from a Biodegradable Copolymer. *Nat. Mater.* **2006**, *5*, 791–796.
23. Qiu, L. Y.; Bae, Y. H. Self-Assembled Polyethylenimine-Graft-Poly(ε-caprolactone) Micelles as Potential Dual Carriers of Genes and Anticancer Drugs. *Biomaterials* **2007**, *28*, 4132–4142.
24. Davis, M. E.; Brewster, M. E. Cyclodextrin-Based Pharmaceutics: Past, Present and Future. *Nat. Rev. Drug Discovery* **2004**, *3*, 1023–1035.
25. Cheng, J. J.; Khin, K. T.; Jensen, G. S.; Liu, A. J.; Davis, M. E. Synthesis of Linear, β-Cyclodextrin-Based Polymers and Their Camptothecin Conjugates. *Bioconjugate Chem.* **2003**, *12*, 1007–1017.
26. Numbenjapon, T.; Wang, J. Y.; Colcher, D.; Schluep, T.; Davis, M. E.; Duringer, J.; Kretzner, L.; Yen, Y.; Forman, S. J.; Raubitschek, A. Preclinical Results of Camptothecin−Polymer Conjugate (IT-101) in Multiple Human Lymphoma Xenograft Models. *Clin. Cancer Res.* **2009**, *15*, 4365–4373.
27. Bartlett, D. W.; Davis, M. E. Physicochemical and Biological Characterization of Targeted, Nucleic Acid-Containing Nanoparticles. *Bioconjugate Chem.* **2007**, *18*, 456–468.
28. Heidel, J. D.; Yu, Z. P.; Liu, J. Y.; Rele, S. M.; Liang, Y. C.; Zeidan, R. K.; Kornbrust, D. J.; Davis, M. E. Administration in Non-human Primates of Escalating Intravenous Doses of Targeted Nanoparticles Containing Ribonucleotide Reductase Subunit M2 siRNA. *Proc. Natl. Acad. Sci. U.S.A.* **2007**, *104*, 5715–5721.
29. Rekharsky, M. V.; Inoue, Y. Complexation Thermodynamics of Cyclodextrins. *Chem. Rev.* **1998**, *98*, 1875–1917.
30. Miyata, K.; Kakizawa, Y.; Nishiyama, N.; Yamasaki, Y.; Watanabe, T.; Kohara, M.; Kataoka, K. Freeze-Dried Formulations for *In Vivo* Gene Delivery of PEGylated Polyplex Micelles with Disulfide Crosslinked Cores to the Liver. *J. Controlled Release* **2005**, *109*, 15–23.
31. Lepecq, J. B.; Paoletti, C. A Fluorescent Complex between Ethidium Bromide and Nucleic Acids Physical—Chemical Characterization. *J. Mol. Biol.* **1967**, *27*, 87–106.
32. Kanayama, N.; Fukushima, S.; Nishiyama, N.; Itaka, K.; Jang, W. D.; Miyata, K.; Yamasaki, Y.; Chung, U.; Kataoka, K. A PEG-Based Biocompatible Block Catiomer with High Buffering Capacity for the Construction of Polyplex Micelles Showing Efficient Gene Transfer toward Primary Cells. *ChemMedChem* **2006**, *1*, 439–444.

33. Wakebayashi, D.; Nishiyama, N.; Itaka, K.; Miyata, K.; Yamasaki, Y.; Harada, A.; Koyama, H.; Nagasaki, Y.; Kataoka, K. Polyion Complex Micelles of pDNA with Acetal-Poly(ethylene glycol)-Poly(2-(dimethylamino)ethyl methacrylate) Block Copolymer as the Gene Carrier System: Physicochemical Properties of Micelles Relevant to Gene Transfection Efficacy. *Biomacromolecules* **2004**, *5*, 2128–2136.
34. Itaka, K.; Yamauchi, K.; Harada, A.; Nakamura, K.; Kawaguchi, H.; Kataoka, K. Polyion Complex Micelles from Plasmid DNA and Poly(ethylene glycol)-Poly(L-lysine) Block Copolymer as Serum-Tolerable Polyplex System: Physicochemical Properties of Micelles Relevant to Gene Transfection Efficiency. *Biomaterials* **2003**, *24*, 4495–4506.
35. Harada, A.; Kataoka, K. Novel Polyion Complex Micelles Entrapping Enzyme Molecules in the Core. 2. Characterization of the Micelles Prepared at Nonstoichiometric Mixing Ratios. *Langmuir* **1999**, *15*, 4208–4212.
36. Kastrup, L.; Oberleithner, H.; Ludwig, Y.; Schafer, C.; Shahin, V. Nuclear Envelope Barrier Leak Induced by Dexamethasone. *J. Cell. Physiol.* **2006**, *206*, 428–434.
37. Rebuffat, A.; Bernasconi, A.; Ceppi, M.; Wehrli, H.; Verca, S. B.; Ibrahim, M.; Frey, B. M.; Frey, F. J.; Rusconi, S. Selective Enhancement of Gene Transfer by Steroid-Mediated Gene Delivery. *Nat. Biotechnol.* **2001**, *19*, 1155–1161.
38. Dames, P.; Laner, A.; Maucksch, C.; Aneja, M. K.; Rudolph, C. Targeting of the Glucocorticoid Hormone Receptor with Plasmid DNA Comprising Glucocorticoid Response Elements Improves Nonviral Gene Transfer Efficiency in the Lungs of Mice. *J. Gene Med.* **2007**, *9*, 820–829.
39. Zingarelli, B.; Sheehan, M.; Wong, H. R. Nuclear Factor-κB as a Therapeutic Target in Critical Care Medicine. *Crit. Care Med.* **2003**, *31*, S105–S111.
40. Daly, W. H.; Poché, D. The Preparation of *N*-Carboxyanhydrides of α-Amino-Acids Using Bis(trichloromethyl) Carbonate. *Tetrahedron Lett.* **1988**, *29*, 5859–5862.
41. Baussanne, I.; Benito, J. M.; Mellet, C. O.; Fernández, J. M. G.; Law, H.; Defaye, J. Synthesis and Comparative Lectin-Binding Affinity of Mannosyl-Coated β-Cyclodextrin-Dendrimer Constructs. *Chem. Commun.* **2000**, 1489–1490.
42. Blout, E. R.; Karlson, R. H. Polypeptides. 3. The Synthesis of High Molecular Weight Poly-γ-L-Glutamates. *J. Am. Chem. Soc.* **1956**, *78*, 941–946.
43. Montaudo, G.; Montaudo, M. S.; Puglisi, C.; Samperi, F. Characterization of Polymers by Matrix-Assisted Laser-Desorption Ionization-Time of Flight Mass Spectrometry-End Group Determination and Molecular-Weight Estimates in Poly(ethylene glycols). *Macromolecules* **1995**, *28*, 4562–4569.
44. Wilhelm, M.; Zhao, C. L.; Wang, Y. C.; Xu, R. L.; Winnik, M. A.; Mura, J. L.; Riess, G.; Croucher, M. D. Polymer Micelle Formation. 3. Poly(styrene-ethylene oxide) Block Copolymer Micelle Formation in Water—A Fluorescence Probe Study. *Macromolecules* **1991**, *24*, 1033–1040.
45. Ringsdorf, H.; Venzmer, J.; Winnik, F. M. Fluorescence Studies of Hydrophobically Modified Poly(*N*-isopropylacrylamides. *Macromolecules* **1991**, *24*, 1678–1686.
46. Chen, V. J.; Smith, L. A.; Ma, P. X. Bone Regeneration on Computer-Designed Nano-fibrous Scaffolds. *Biomaterials* **2006**, *27*, 3973–3979.